ELSEVIER

International Journal of Mass Spectrometry 223–224 (2003) 335–342

International Journal of Mass Spectrometry

www.elsevier.com/locate/ijms

Vibrational relaxation in $H_2 + H_2$: full-dimensional quantum dynamical study

Sergei K. Pogrebnya, Margot E. Mandy[1], David C. Clary[*]

Department of Chemistry, University College London, 20 Gordon Street, London WC1H 0AJ, UK

Received 5 January 2002; accepted 21 May 2002

Abstract

A full-dimensional quantum dynamical study of vibrational relaxation in $H_2 + H_2$ collisions using the potential energy surface (PES) of Schwenke is reported. The essential role of the anisotropy of the interaction potential is elucidated. A comparison of theoretical and experimental rate coefficients is made. (Int J Mass Spectrom 223–224 (2003) 335–342)

Keywords: Non-elastic scattering; Potential energy surface; Vibrational relaxation

1. Introduction

Hydrogen is the most abundant molecule in the universe. Knowledge of inelastic state-to-state rate coefficients in $H_2 + H_2$ collisions is of fundamental importance for understanding and modelling the energy balance in the interstellar medium [1]. The first rigorous quantum scattering studies on the pure rotational excitations in $H_2 + H_2$ collisions were made more that two decades ago [2,3]. In these calculations a diatomic molecule was treated as a rigid rotor. Nowadays such calculations can be performed rather routinely [4], provided the potential energy surface (PES) is expanded in an appropriate series of spherical harmonics. More recently, quantum scattering calculations incorporating vibrational degrees of freedom have started to emerge [5,6]. However, in these calculations a vibrational degree of freedom only of one H_2 molecule was treated explicitly and the second H_2 molecule was treated as a rigid rotor either in the ground rotational state [5] or including three lowest rotational states [6]. The process of the vibrational relaxation in collisions between H_2 molecules also has been studied using semiclassical methods (see, for example [7], and references cited therein).

In the present letter we perform full-dimensional quantum scattering calculations of rovibrational state-to-state cross-sections and rate coefficients for the $H_2 + H_2$ system. We use an approach, which permits the calculations to be done on a PES of any functional form. We also examine how the results are sensitive to a choice of PES. A comparison with experimental results as well as other theoretical results is also made.

[*] Corresponding author. E-mail: d.c.clary@ucl.ac.uk

[1] Present address: Program in Chemistry, University of Northern British Columbia, Prince George, BC, Canada V2N 4Z9.

1387-3806/02/$ – see front matter
PII S1387-3806(02)00869-2

2. Theory

The quantum formulation of the collision between two diatomic molecules is well documented. Since all relevant details can be found in [2,3,8–10], and references cited therein, only a brief outline is given here. In general, we follow the formulation given by Alexander and DePristo [10]. We use a body-fixed (BF) coordinate system, the BF Z-axis pointing along the vector $\boldsymbol{R}$, which connects the centre of mass of the two molecules. The BF internal coordinates are R, r_1, r_2, θ_1, θ_2, ϕ. Here $R = |\boldsymbol{R}|$, r_i is the length of the vector $\boldsymbol{r}_i$ connecting the atoms in molecule i, $\cos\theta_i = \boldsymbol{r}_i \cdot \boldsymbol{R}/r_i R$, and ϕ is the torsion angle between vectors $\boldsymbol{r}_1$ and $\boldsymbol{r}_2$.

The rotational angular momenta of two molecules $\boldsymbol{j}_1$ and $\boldsymbol{j}_2$ are coupled to form $\boldsymbol{j}_{12}$, which is subsequently coupled to the orbital angular momentum $\boldsymbol{L}$ to form the total angular momentum $\boldsymbol{J}$. The projection of $\boldsymbol{J}$ on the space-fixed and BF Z-axis are M and Ω, respectively. The total wave function is expanded as

$$\Psi(\boldsymbol{r}_1, \boldsymbol{r}_2, \boldsymbol{R}) = R^{-1} \sum_{v,j,J,M,\Omega,\varepsilon} F^{JM\varepsilon}_{vj\Omega}(R)\psi^{JM\varepsilon}_{vj\Omega}(\boldsymbol{r}_1, \boldsymbol{r}_2), \tag{1}$$

where

$$\psi^{JM\varepsilon}_{vj\Omega}(\boldsymbol{r}_1, \boldsymbol{r}_2) = \chi_{v_1 j_1}(r_1)\chi_{v_2 j_2}(r_2)|JMj\Omega\varepsilon\rangle. \tag{2}$$

Here v denotes vibrational quantum numbers (v_1, v_2), j stands for (j_1, j_2, j_{12}), ε is the spatial inversion parity, $\chi_{v_i j_i}(r_i)$ is the rovibrational wave function of molecule i, and $|JMj\Omega\varepsilon\rangle$ is the BF rotational wave function. The latter is the eigenfunction for J, j_1, j_2, j_{12}, Ω, and the spatial parity operator. The explicit form of the BF functions $|JMj\Omega\varepsilon\rangle$ can be found elsewhere [10,11]. With the expansion Eq. (1), the total Schrödinger equation is transformed into the usual set of BF close-coupling (CC) equations [10,11]. In the BF frame, matrix elements of the $(\boldsymbol{J} - \boldsymbol{j}_{12})^2$ operator are diagonal in all quantum numbers but Ω. Here we utilise the coupled states approximation (CSA) [12,13], which neglects the coupling between states with different Ω.

It is important to note that interchange symmetry must be taken into account when dealing with two identical molecules [2,3,8–10]. Following Alexander and DePristo [10], in this case, we use the symmetrised functions

$$\psi^{JM\varepsilon p}_{vj\Omega} = \Delta_{vj_1j_2}[\psi^{JM\varepsilon}_{vj\Omega} + p\varepsilon(-1)^{j_{12}}\psi^{JM\varepsilon}_{\bar{v}\bar{j}\Omega}], \tag{3}$$

where $p = \pm 1$ is the molecule interchange parity, $\bar{v} = (v_2, v_1)$, $\bar{j} = (j_2, j_1, j_{12})$, and

$$\Delta_{vj_1j_2} = [2(1 + \delta_{v_1v_2}\delta_{j_1j_2})]^{-1/2}. \tag{4}$$

We also require $v_1 < v_2$, or $v_1 = v_2$ and $j_1 \leq j_2$ ("well ordered states") to ensure that the basis set is linearly independent.

In the BF frame, the calculation of potential energy matrix elements involves evaluation of integrals of the type

$$\begin{aligned} U^{\Omega}_{vv'jj'}(R) = \langle &\chi_{v_1j_1}\chi_{v_2j_2}Y^{j_{12}\Omega}_{j_1j_2} \\ &\times |V_{\text{int}}(r_1, r_2, \theta_1, \theta_2, \phi; R)| \\ &\times \chi_{v'_1j'_1}\chi_{v'_2j'_2}Y^{j'_2\Omega}_{j'_1j'_2}\rangle, \end{aligned} \tag{5}$$

where

$$\begin{aligned} Y^{j_{12}\Omega}_{j_1j_2} = &\sum_m \langle j_1 m j_2 \Omega - m|j_{12}\Omega\rangle y^m_{j_1} \\ &\times (\theta_1, 0)y^{\Omega-m}_{j_2}(\theta_2, \phi), \end{aligned} \tag{6}$$

where $y^m_j(\theta, \phi)$ are spherical harmonics, and V_{int} is the interaction potential. The latter is defined as a difference between the total PES of the system and the sum of potentials corresponding to free diatomics, $V_i(r_i)$. We use the potential optimised discrete variable representation (PO-DVR) [14] to construct rovibrational basis functions $\chi_{v_i j_i}(r_i)$ and calculate rovibrational energies of a diatom, $E_{v_i j_i}$, as was described previously in the case of atom–diatom collisions [15]. This allows us to perform the integration over r_1 and r_2 in a simple and efficient way. In principle, integration over angles θ_1, θ_2, ϕ can be done analytically provided the potential is expanded over spherical harmonics. However, in this study we adopt a numerical approach and use Gauss–Legendre points to integrate over θ_1 and θ_2, and Gauss–Chebyshev ones to integrate over ϕ.

This allows us to perform the calculations using a PES of an arbitrary functional form.

A set of coupled states equations is solved numerically subject to appropriate boundary conditions. These boundary conditions define elements of the ***S***-matrix and hence the state-to-state cross-sections given by [8]

$$\sigma^{\varepsilon p}(\gamma\to\gamma';E_c)=\frac{\pi(1+\delta_{v_1v_2}\delta_{j_1j_2})(1+\delta_{v_1'v_2'}\delta_{j_1'j_2'})}{(2j_1+1)(2j_2+1)k_{\gamma\gamma}^2}\times\sum_{J\Omega j_{12}j_{12}'}(2J+1)|\delta_{vv'jj'}-S_{vv'jj'}^{J\Omega\varepsilon p}|^2, \tag{7}$$

where $\gamma=(v_1,j_1,v_2,j_2)$, $k_{\gamma\gamma}^2=(2\mu/\hbar^2)(E-E_{v_1j_1}-E_{v_2j_2})$, E is the total energy, $E_c=E-E_{v_1j_1}-E_{v_2j_2}$ is the collision (translation) energy, and μ is the reduced mass.

3. Results and discussions

In this first implementation, we consider a particular case of transitions from the ground rotational state, i.e.,

$$H_2\,(v_1,j_1=0)+H_2\,(v_2,j_2=0)\to H_2\,(v_1',j_1')+H_2\,(v_2',j_2'). \tag{8}$$

When $j_1=j_2=0$, j_{12} must equal zero and $\Omega=0$. In this case the inversion parity is well defined and given by $\varepsilon=(-1)^J$ [10].

To test part of the computational scheme, we calculated pure rotational excitation cross-sections for the interaction potential of Farrar and Lee as modified by Zarur and Rabitz (FLZR) [16]. The calculations were performed using the rotational basis set j_1, $j_2=0$, 2, 4, $j_1\le j_2$. In this case the bond length of each H_2 molecule was fixed to its equilibrium value, $r_1=r_2=1.449a_0$, and the rotational energy of the ith rotor is given by $E_{j_i}=B_e j_i(j_i+1)$ with $B_e=60.8\,cm^{-1}$. Table 1 compares the results of these test calculations with the results obtained by using the MOLSCAT program [4]. One sees that our CSA results practically are nearly identical to MOLSCAT, CSA ones, and in very good agreement with those obtained with CC method.

Now we proceed to the full-dimensional calculations for the vibrational relaxation process: $(v_1=0,j_1=0,v_2=1,j_2=0)\to(v_1'=0,j_1',v_2'=0,j_2')$. The calculations were performed using the "well ordered" basis set: $v_2=0$, 1, 2, for each v_2 $j_2=0,\ldots,j_{max}^v$, for $v_1<v_2$ $j_1=0,\ldots,j_{max}^v$, and for $v_1=v_2$ $j_1=0,\ldots,j_2$. Values for j_{max}^v are 10, 8, 2 for $v=0$, 1, 2, respectively. Rovibrational functions of the H_2 molecule were obtained with the $V_{H_2}(r)$ potential of Schwenke [18]. For a given PES, the set of coupled states equations was solved using the R-matrix propagation method [17], starting from $R_{min}=1a_0$ and integrating out to $R_{max}=40a_0$. We used five PO-DVR points to integrate over r_1 and r_2, respectively. These parameters, as well as the size of the grid $24\times24\times24$ to integrate over angles θ_1, θ_2, and ϕ, were determined by performing appropriate convergence tests.

Initially we performed the calculations on the PES developed by Schwenke [18]. This H_2–H_2 interaction potential (hereafter referred as SW) is a fit to ab initio

Table 1
State-to-state cross-sections (in a.u.) for the $H_2\,(0,0)+H_2\,(0,0)\to H_2\,(0,j_1)+H_2\,(0,j_2)$ collisions on the FLZR potential energy surface

E_c (eV)	(j_1,j_2)	Present	MOLSCAT, CSA	MOLSCAT, CC
0.15	0, 2	0.1747 (+01)	0.1766 (+01)	0.1679 (+01)
	2, 2	0.5645 (−01)	0.5580 (−01)	0.5529 (−01)
0.30	0, 2	0.4275 (+01)	0.4302 (+01)	0.4116 (+01)
	2, 2	0.2577 (+00)	0.2576 (+00)	0.2479 (+00)
	0, 4	0.1151 (−01)	0.1151 (−01)	0.1109 (−01)
	2, 4	0.6315 (−03)	0.6280 (−03)	0.7027 (−03)

Numbers in parentheses are powers of 10.

data and has the functional form

$$V_{\rm int} = [V_{\rm P}(R_{\rm AC}) + V_{\rm P}(R_{\rm AD}) + V_{\rm P}(R_{\rm BC}) + V_{\rm P}(R_{\rm BD})] \times F_{\rm C}(R, r_1, r_2, \theta_1, \theta_2, \phi) + V_{\rm LR}(R, r_1, r_2, \theta_1, \theta_2, \phi). \quad (9)$$

Here $V_{\rm P}(R_{ij})$ is the pairwise potential depending on distances between non-bonding H atoms, $F_{\rm C}$ is the correction function, and $V_{\rm LR}$ is the long range potential. It is important to note that both $F_{\rm C}$ and $V_{\rm LR}$ are represented by the expansion over functions

$$\Phi_{q_1q_2\mu}(\theta_1, \theta_2, \phi) = \frac{4\pi}{[2(1+\delta_{\mu_0})]^{1/2}}[y^{\mu}_{q_1}(\theta_1, 0) y^{-\mu}_{q_2}(\theta_2, \phi) + y^{-\mu}_{q_1}(\theta_1, 0) y^{\mu}_{q_2}(\theta_2, \phi)], \quad (10)$$

with the expansion coefficients being dependent on R, r_1, r_2. Although these expansions were restricted to $q_1, q_2 \leq 2$, the presence of the pairwise potentials ensures that higher order anisotropies exist. It was pointed out by Flower and Roueff [5] that the SW potential features a surprising behaviour, i.e., the interaction becomes more anisotropic as R increases. Therefore, in the subsequent calculations [5,6] they used the interaction potential of a form

$$V^{\rm F}_{\rm int} = \sum_{q_1q_2\mu} A_{q_1q_2\mu}(r_1, r_2, R)\Phi_{q_1q_2\mu}(\theta_1, \theta_2, \phi), \quad (11)$$

which contains only the terms with $q_1, q_2 \leq 2$ (only even values of $q_{1,2}$ give a contribution as H_2 is homonuclear). It should be noted that the fit (9) was based on the results of ab initio calculations performed for five different geometries. In principle, the set of five geometries enables only the five terms with $q_1, q_2 \leq 2$ in the angular expansion to be determined. Therefore, we consider the existence of higher anisotropies in the fit (9) to be rather questionable. Bearing this in mind, we also performed calculations with the potential $V^{\rm exp}_{\rm int}$ (SWE), which is obtained by expanding potential (9) over functions $\Phi_{q_1q_2\mu}$ restricted to $q_1, q_2 \leq 2$. We would like to stress that the difference between SW and SWE potentials is rather small, as is illustrated in Table 2. However, we will see that this results in a significant effect in vibrational relaxation cross-sections.

Table 2
Values of the SW and the SWE interaction potentials (in a.u.) calculated at $\theta_1 = \theta_2 = \pi/4$, $\phi = 0$, as a function of R

R (a_0)	SW potential	SWE potential
2.5	0.1019 (+00)	0.9970 (−01)
3.0	0.4782 (−01)	0.4646 (−01)
4.0	0.8949 (−02)	0.8641 (−02)
5.0	0.1301 (−02)	0.1208 (−02)
7.0	−0.1542 (−03)	−0.1520 (−03)
10.0	−0.2088 (−04)	−0.2088 (−04)

Numbers in parentheses are powers of 10.

Fig. 1 gives a comparison of initial rotational state-selected cross-sections, $\sigma_{00} = \sum_{j_1'j_2'}\sigma(0, 0, 1, 0 \rightarrow 0, j_1', 0, j_2')$, as a function of the collision energy, calculated using potentials SW and SWE, respectively. One sees that at high collision energies the difference between two sets of calculations is small. However, it becomes considerable as the collision energy decreases. To understand such a behaviour, we present (Fig. 2a and b) state-to-state cross-sections, $\sigma_{00j_1'j_2'} = \sigma(0, 0, 1, 0 \rightarrow 0, j_1', 0, j_2')$, at collision energies 0.01 and 0.5 eV. The efficiency of the transition to the particular rotational state is determined by a competition between the energy gap effect that favours the transition with small ΔE and the combined influence of rotational coupling and angular momentum conservation, which favour small Δj_i. At small collision energies the high anisotropy of potential (9) results in strong rotational coupling and makes the transitions to highly excited rotational states to be very efficient, the near-resonant transition $(0, 0, 1, 0) \rightarrow (0, 0, 0, 8)$ ($\Delta E \approx 100\,{\rm cm}^{-1}$) being dominant. That is not the case when the less anisotropic SWE potential is used. For this potential, due to the restriction $q_1, q_2 \leq 2$ the direct coupling between states with $|\Delta j_i| > 2$ does not exist and that results in low populations of states with high j_i. At higher collision energies both potentials give similar product distributions, although the use of potential (9) still results in greater populations of highly excited rotational states as compare with those obtained using the SWE potential.

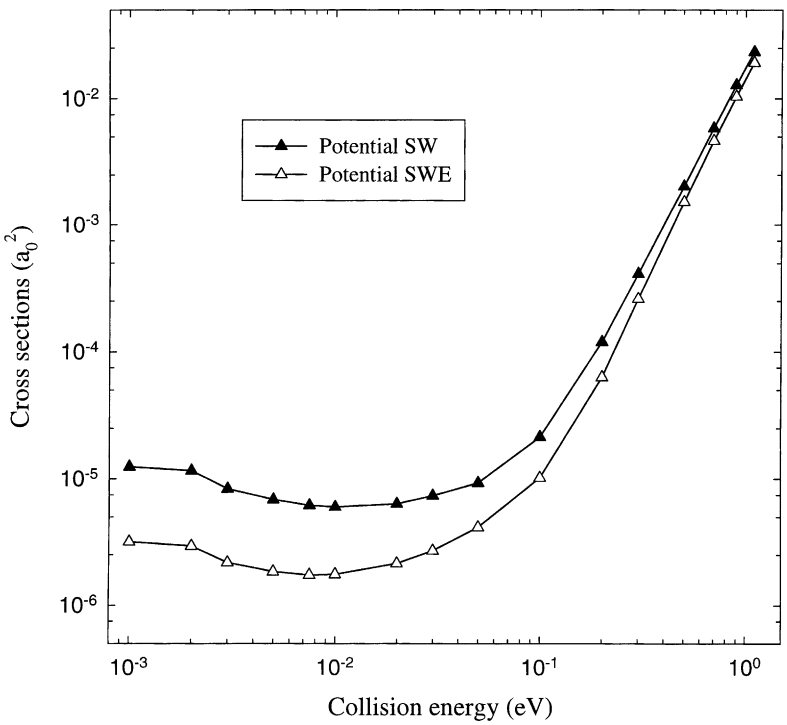

Fig. 1. Initial state-selected cross-sections, $\sigma(0, 1, 0, 0 \rightarrow 0, 0, \text{all } j_1', j_2')$, as a function of the collision energy calculated with potentials SW and SWE, respectively.

By averaging cross-sections $\sigma_{00}(E_c)$ over the Maxwell–Boltzmann distribution we find initial state-selected vibrational relaxation rate coefficients $k_{00}(T) = k(v = 1, j_1 = 0, j_2 = 0 \rightarrow v' = 0; T)$. In Table 3, we compare the rate coefficients, $k_{00}(T)$, obtained using SW and SWE potentials, respectively, with those based on the results of [6]. The latter were calculated as a sum of corresponding state-to-state rate coefficients reported in [6]. One may see that our results calculated on the SWE potential surface are in quite good agreement with those calculated by Flower [6]. The use of the SW potential increases $k_{00}(T)$ by a factor of about 2 at $T = 300$–500 K. To make a direct comparison with the experimental data, one needs to determine the total rate coefficients, $k(T) \equiv k(v = 1 \rightarrow v' = 0; T)$. That requires $k_{j_1 j_2}(T)$ to be calculated for different initial j_1 and j_2 and $k(T)$ is then obtained by weighting the initial state-selected rate coefficients by the relative populations of initial levels according to the Boltzmann distribution. At low temperatures ($T < 100$ K) populations of rotationally excited initial states of H_2 are negligible and only $k_{00}(T)$ needs to be calculated to obtain the total rate coefficient. The previous studies of the vibrational relaxation in atom–molecule systems [15,19] show that $k_{00}(T)$ provides a reliable estimation of $k(T)$ for temperatures up to $T \cong 300$ K. This is also confirmed by

Table 3
Rate coefficients $k_{00}(T)$ and $k(T)$ (in $cm^3\,s^{-1}$)

T (K)	k_{00}, SW	k_{00}, SWE	k_{00} [6][a]	k [6]
100	2.9 (−17)	9.4 (−18)	–	6.4 (−18)[b]
300	9.1 (−17)	4.0 (−17)	3.3 (−17)	4.6 (−17)
500	3.2 (−16)	1.7 (−16)	1.2 (−16)	3.3 (−16)

Numbers in parentheses are powers of 10.

[a] Calculated as the sum of corresponding state-to-state rate coefficients reported in [6].

[b] Reported in [5].

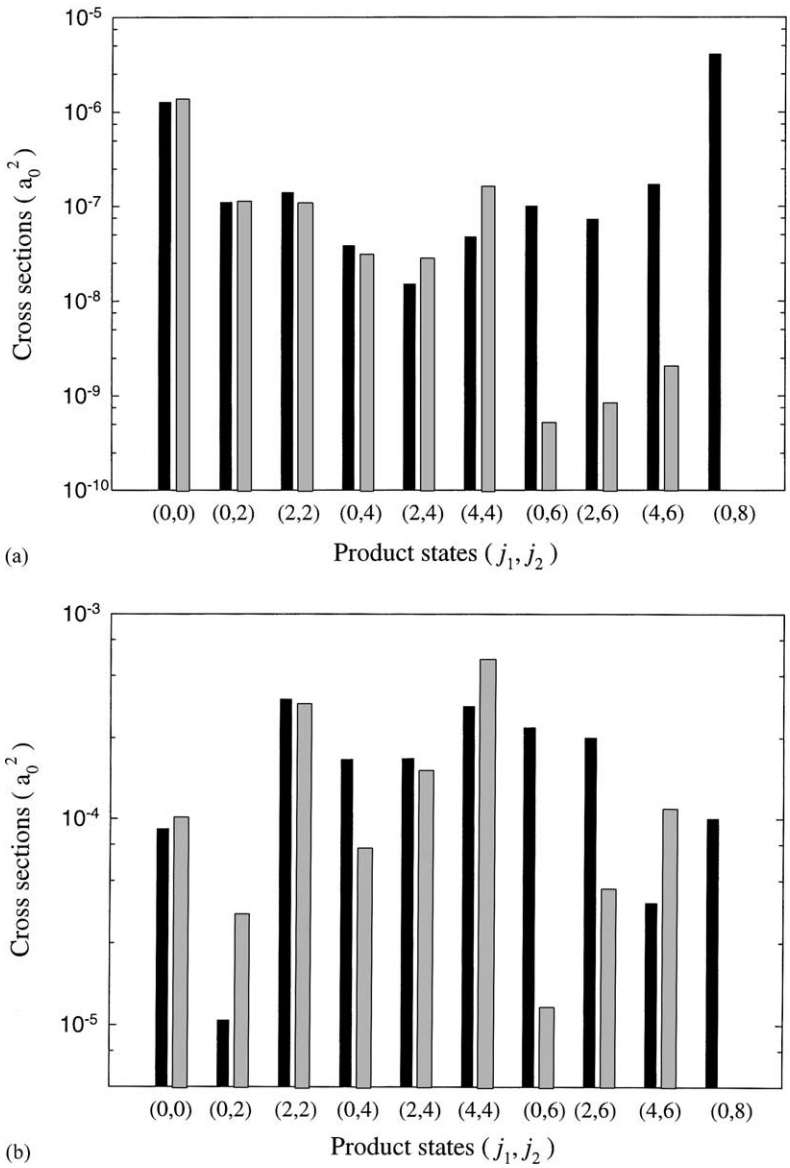

Fig. 2. (a) State-to-state cross-sections calculated with the SW potential (black bars) and with the SWE potential (grey bars) at $E_c = 0.01$ eV. (b) The same as part a but $E_c = 0.5$ eV.

the results of [6] given in Table 3. We see that at $T = 300$ K, $k(T)/k_{00}(T) \cong 1.4$. Of course, as the temperature increases $k_{00}(T)$ provides a less accurate estimation of $k(T)$ and at $T = 500$ K, $k(T)/k_{00}(T) \cong 2.8$.

Fig. 3 gives a comparison of $k_{00}(T)$, as a function of the temperature, calculated using SW and SWE potentials, respectively, with the experimental results for *para*-H_2 [20]. We see that at low temperatures, the results based on a less anisotropic SWE potential are in better agreement with the experimental data than those obtained using the SW potential. As described above, this is due to the strong anisotropy of the SW

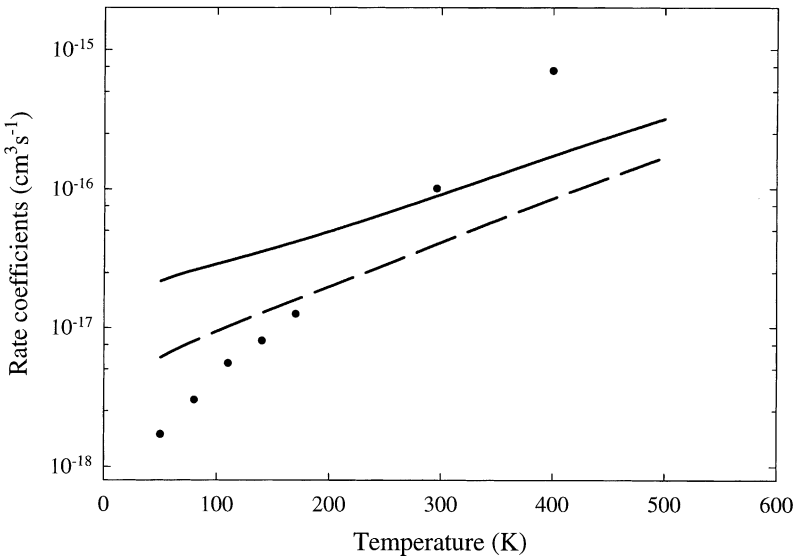

Fig. 3. Rate coefficients for vibrational relaxation of *para*-H_2 calculated on the SW (solid line) and the SWE (dashed line) potentials, respectively, in comparison with the experimental data of [20] (circles).

potential, which allows the coupling between the initial state (0, 0, 1, 0) and the near-resonant state (0, 0, 0, 8), and the corresponding transition gives a main contribution to $\sigma_{00}(E_c)$ at low collision energies. The results suggest that the global fit of Schwenke [18] is preferable to the SWE potential and the potential used in [6] for $T \geq 300$ K. However, at such temperatures $k_{00}(T)$ provides only a lower estimate for the total rate coefficient and, therefore, rotationally excited initial states of H_2 must be taken into consideration to obtain a definitive conclusion.

We would like to note that the results of semiclassical calculations [7] were reported to be in a good agreement with the experimental data over the temperature range 50–2000 K. These results were obtained on a different PES [21] which is also based on the ab initio energies of Schwenke [18]. Therefore, bearing in mind that the results of quantum scattering calculations are very sensitive to the choice of the PES, the comparison between quantum and semiclassical results will make sense only if both sets of calculations are performed on the same surface. This will be the subject of a future study.

4. Conclusion

We have shown that the anisotropy of the interaction potential has a significant influence on the outcome of quantum dynamical calculations for the vibrational relaxation in the $H_2 + H_2$ system. Our results suggest the potential energy fit developed by Schwenke [18] is adequate to describe rate coefficients at temperatures in the range of 300–500 K. However, the use of this potential overestimates considerably the experimental rate coefficient at lower temperatures. Our full-dimensional results obtained on a less anisotropic potential SWE are consistent with the results of five dimensional calculations [6] based on a similar potential surface. Using the SWE potential improves the agreement with the experimental data at low temperatures but tends to underestimate rate coefficients at higher temperatures. Since vibrational relaxation in $H_2 + H_2$ is an important process accessible both by theory and experiment, further improvements in the $H_2 + H_2$ PES are desirable. Calculations of inelastic cross-sections for collisions between *para* and *ortho* H_2 molecules based

on a newly developed PES [22] are currently being done.

Acknowledgements

This work was supported by Engineering and Physical Sciences Research Council (UK) as well as the Natural Sciences and Engineering Research Council of Canada. Some of the calculations were carried out using the high performance computing facility jointly supported by the Canadian Foundation for Innovation, the British Columbia Knowledge Development Fund, and Silicon Graphics at the University of Northern British Columbia.

References

[1] A. Sternberg, A. Dalgarno, Astrophys. J. 338 (1989) 197.
[2] S. Green, J. Chem. Phys. 62 (1975) 2271.
[3] T.G. Heil, S. Green, D.J. Kouri, J. Chem. Phys. 68 (1978) 2562.
[4] J.M. Hutson, S. Green, MOLSCAT Computer Code, Version 14, Distributed by Collaborative Computational Project No. 6 of the Engineering and Physical Sciences Research Council, UK, 1994.
[5] D.R. Flower, E. Roueff, J. Phys. B: Atm. Mol. Opt. Phys. 31 (1998) 2935.
[6] D.R. Flower, J. Phys. B: Atm. Mol. Opt. Phys. 33 (2000) 5243.
[7] V.A. Zenevich, G.D. Billing, J. Chem. Phys. 111 (1999) 2401.
[8] K. Takayanagi, Adv. Atm. Mol. Phys. 1 (1965) 149.
[9] H. Rabitz, J. Chem. Phys. 63 (1975) 5208.
[10] M.H. Alexander, A.E. DePristo, J. Chem. Phys. 66 (1977) 2166.
[11] J.-M. Launay, J. Phys. B: Atm. Mol. Phys. 10 (1977) 3665.
[12] R.T. Pack, J. Chem. Phys. 60 (1974) 633.
[13] P. McGuire, D.J. Kouri, J. Chem. Phys. 60 (1974) 2488.
[14] J. Echave, D.C. Clary, Chem. Phys. Lett. 190 (1992) 225.
[15] S.K. Pogrebnya, A.K. Kliesch, D.C. Clary, M. Cacciotore, Int. J. Mass Spectrom. Ion Process. 149/150 (1995) 207.
[16] G. Zarur, H. Rabitz, J. Chem. Phys. 60 (1974) 2057.
[17] E.B. Stechel, R.B. Walker, J.C. Light, J. Chem. Phys. 69 (1978) 3518.
[18] D.W. Schwenke, J. Chem. Phys. 89 (1988) 2076.
[19] A.J. Banks, D.C. Clary, J. Chem. Phys. 88 (1987) 802.
[20] M.-M. Audibert, R. Vilaseca, J. Lukasik, J. Ducuing, Chem. Phys. Lett. 31 (1975) 232.
[21] G.D. Billing, R.E. Kolesnick, Chem. Phys. Lett. 215 (1993) 571.
[22] A.I. Boothroyd, P.G. Martin, W.J. Keogh, M.R. Peterson, J. Chem. Phys. 116 (2002) 666.